# INORGANIC NANOPARTICLES FOR ELECTROCHEMICAL APPLICATIONS SYNTHESIZED USING SUPERCRITICAL CARBON DIOXIDE

I. V. Elmanovich*[a,b,c]

[a] *Nesmeyanov Institute of Organoelement Compounds, Russian Academy of Sciences, ul. Vavilova 28, Moscow, 119991 Russia*
[b] *Faculty of Physics, Lomonosov Moscow State University, Leninskie Gory 1, str. 2, Moscow, 119991 Russia*
[c] *Semenov Federal Research Center for Chemical Physics, Russian Academy of Sciences, ul. Kosygina 4, str.1, Moscow, 119991 Russia*

Cite this: *INEOS OPEN*, **2020**, *3 (5)*, 165–171
DOI: 10.32931/io2021r

*Received 25 September 2020,*
*Accepted 15 October 2020*

http://ineosopen.org

## Abstract

The review briefly outlines some of the main areas of using supercritical carbon dioxide in the synthesis and modification of functional materials for electrochemical applications. The synthesis of supported metal nanoparticles as well as metal oxide nanoparticles/aerogels and modification of polymer electrolyte membranes are considered. This work attempts to highlight the key benefits associated with the supercritical state of the solvent specifically for every listed application.

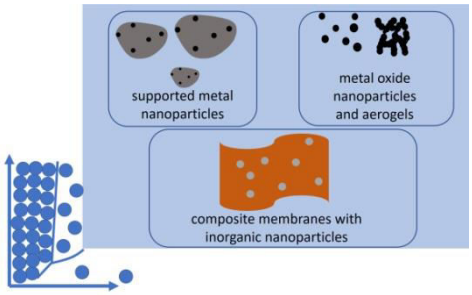


**Key words:** supercritical carbon dioxide, nanoparticles, aerogels, polymer electrolyte membranes.

## Introduction

The use of supercritical $CO_2$ (sc $CO_2$) for the synthesis and characterization of functional materials for various applications has been attracting the steady interest of researchers during the past few decades. Quite a distinctive combination of physical and chemical properties of sc $CO_2$ can provide certain benefits in the polymer synthesis and modification, extraction, impregnation, and separation processes as well as in the synthesis of nanoparticles of various chemical nature. Carbon dioxide is relatively nontoxic, abundant, and inexpensive; it is a suitable solvent for a wide range of organic compounds and some classes of polymers. Perhaps the most important feature of sc $CO_2$ as a medium is that, being a supercritical fluid, it does not form a phase boundary in a vessel and, thus, provides some unique opportunities for the modification of porous substrates. Indeed, the absence of any surface-tension-driven effects as well as the elimination of a residual solvent problem might be considered crucial benefits when working with fine porous structures. It is no coincidence, for example, that it was the implementation of supercritical fluids that allowed for the synthesis of one of the most marvelous porous materials that we have at hand—the aerogels.

In the scope of possible uses of sc $CO_2$ in research and development, of particular note are the functional materials for electrochemical applications. Electrochemical power sources (EPS), such as fuel cells, Li-ion batteries, or vanadium redox flow batteries, are the devices in which free energy change associated with a particular redox chemical reaction can be stored and potentially converted to useful energy output. Generally, the most important structural elements of any EPSs are electrodes and ion-conducting membrane. Selective ion conductivity of the membrane, efficient catalysis, electron, and mass transport throughout the electrodes, as well as the formation of an optimal boundary between the two main components need to be taken into consideration when designing a new EPS. Consequently, a membrane electrode assembly is usually a rather complex composite *porous* structure, which development and fabrication require the consideration of many factors. For example, the problems of residual solvent traces that can "poison" sensitive electrode reactions as well as capillary forces that can collapse the structures of electrodes or a membrane, leading to the decreased surface area or disrupted electron, ion or mass transport, are ever present. Hence, the use of sc $CO_2$ for the synthesis and modification of functional materials for electrochemical applications is of paramount interest.

The present review outlines two domains of the use of sc $CO_2$ for electrochemical applications: the preparation of electrode materials and modification of ion-conducting membranes. In particular, metal and metal oxide nanoparticles, as well as aerogel-based composites are considered for the electrode materials. Regarding membrane modification, various approaches towards the modification of ion-conducting membranes with inorganic nanoparticles are described and compared. The aim of this study is not to yield a complete analysis of all the existing research on the matter but to highlight the key aspects that make sc $CO_2$ a unique fit for the considered purposes.

## Metal nanoparticles for electrocatalysis

### Method basics

Supercritical fluid deposition approach for the formation of supported metal nanoparticles (SFDm) was first presented in the pioneer work of J. J. Watkins and T J. McCarthy in 1995 [1].

The work featured dimethyl(1,5-cyclooctadiene)platinum ($PtMe_2(COD)$) as a platinum precursor and two types of substrates: polytetrafluoroethylene (PTFE) and poly(4-methyl-1-pentene) (PMP). The general synthetic route is schematically described in Fig. 1.

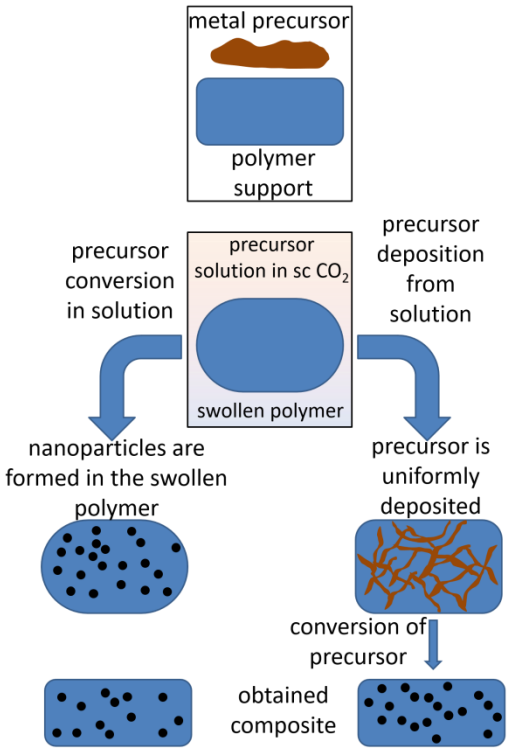


**Figure 1**. General synthetic approach to supported metal nanoparticles presented by J. J. Watkins and T. J. McCarthy in Ref. [1].

At the first step, a polymer support and a suitable precursor are placed in a high-pressure autoclave. The reactor is filled with $CO_2$, after which the precursor goes into solution and the polymer swells. Further, the course of synthesis can be directed along several paths: either the conversion of the precursor can be carried out directly in the supercritical solution or, after reaching thermodynamic equilibrium in the solution, the isothermal expansion of $CO_2$ can result in the formation of a polymer composite containing the metal precursor. In the latter case, a final step is necessary, during which the conversion of the precursor will be carried out in the said polymer composite. In turn, the conversion procedure itself can be achieved through both chemical (for $PtMe_2(COD)$, such a chemical conversion can be achieved *via* hydrogenolysis) and thermally induced transformation. However, below we will show that a combination of these approaches can also be effective. Apart from the general concept, the work [1] presented the first results: it turns out that the formed Pt nanoparticle clusters are smaller if the precursor is converted after the deposition rather than in the supercritical solution. Further, for the amorphous PMP, a uniform distribution of Pt nanoparticles was detected both on the surface and in the bulk of the material. For PTFE, the Pt concentration in the bulk was significantly smaller; however, the very presence of metal inside such a highly crystalline polymer, for which processing in any chemical solvent is a non-trivial task in itself, is an important result demonstrating the potential of using sc $CO_2$ as a medium for the formation of metal-polymer composites.

Possible combinations of the chemical nature of the metal and substrate (Pt@PMP and Pt@PTFE) proposed in the pioneering work were subsequently significantly expanded. Indeed, there are examples of using SFDm for the synthesis of nanoparticles of platinum [2–4], palladium [5, 6], silver [7], ruthenium [6], nickel [8], and bimetallic complexes [9]. Porous polymers [2, 7], conducting carbon substrates [5, 6], and aerogels of various chemical nature [2, 4] were used as possible supporting materials. The works of the first decade of the SFDm development were analytically reviewed by C. Erkey and colleagues [10]. The same scientific group has released one of the most relevant reviews on this topic to date [11]. In another extensive recent review on SFDm by Barim *et al.* [12], the authors state that, although the experimental data on supercritical deposition is vast, further investigation of the phase behavior of multicomponent systems consisting of $CO_2$ and metal precursors along with computational and theoretical studies can greatly improve our understanding of the process.

## Supported Pt nanoparticles as cathode materials

The main reason for the use of SFDm for the preparation of materials for electrochemical applications is the synthesis of electrocatalysts for fuel cell electrodes based on supported electrocatalytic nanoparticles. In particular, the use of Pt as a catalyst provides unique efficiency of an oxygen reduction reaction in an acidic environment, which is crucial for the cathode operation of hydrogen/oxygen fuel cells. Further, Pt-containing cathode catalysts, which are expensive and subject to relatively rapid degradation, are an economic bottleneck that prevents widespread adoption of these devices [13]. For more efficient utilization of Pt nanoparticles (NPs) rather than individual nanoparticles, usually some composite material is used, in which metal NPs are deposited on a dispersed electrically conducting support carrier, most often based on carbon. Thus, the motivation for using the SFDm process in the synthesis of these dispersed systems is twofold. At the deposition stage, the use of a supercritical fluid enables uniform delivery of the precursor to pores of any diameter in the substrate material owing to the absence of capillary forces. In addition, at the stage of solvent removal, $CO_2$ is converted to a gas phase, completely leaving the modified dispersed phase without a residue. In order to prevent the formation of a liquid phase at any stage of the process, the quasi-equilibrium isothermal expansion of $CO_2$ at the temperature above the critical one is implemented. The uniformity of the modification should ensure both the formation of relatively monodisperse platinum particles as a result of the conversion and a uniform coating of the surface of the electron-conducting carrier by these monodisperse nanoparticles.

The first works in which SFDm was used to obtain electrocatalysts for fuel cells were published in the mid-2000s [14–16]. For the composite materials obtained, not only the compositions, surface structures, and morphologies but also the electrocatalytic activities were explored. The electrocatalysts were studied both in model electrochemical half cells with a rotating disk electrode [17] and in operating fuel cells [18].

Various types of carbons, including carbon black, carbon nanotubes, and carbon aerogels, were used as conductive substrates. Even though the problem of a residual solvent is eliminated when using SFD, the problem of ligand traces that can hinder the catalytic process still remains. Said-Galiev *et al*. noted [19] that the complete conversion of a precursor is the key to obtaining efficient electrocatalytic materials. Moreover, the analysis of the degree of conversion is in itself a methodological challenge since both gravimetric and spectroscopic methods bare certain experimental errors. In the case of gravimetric measurements, where a change in the mass during precursor decomposition is studied, there is a possibility of the mass change due to supercritical extraction of some organic traces or residual water from the substrate during the decompression stage. Concerning the spectroscopic methods, it is known that the interaction of organometallic compounds and electrons with energies as low as 50 eV can cause the decomposition of these compounds [20]. The latter is also a challenge for imaging techniques that use electron beams, such as transmission electron microscopy (TEM) and scanning electron microscopy (SEM). Our research group presented [21] a model experiment that utilized scanning force microscopy (SFM) to visualize different stages of the formation of Pt nanoparticles using highly oriented pyrolytic graphite (HOPG) as a substrate. SFM is a "non-destructive" visualization method for which the study of "soft" polymer, biopolymer or organic structures is considered to be the niche applications.

The resulting SFM images are presented in Fig. 2. Image **a** is a $PtMe_2$(COD) thin film (1.6–2.1 nm in height) deposited onto the HOPG surface. Note, that there are some characteristic features of the substrate itself: lines can be seen in the images, sometimes a change in the contrast of the image is observed near the lines. This is due to some topographic defects of the HOPG surface, the simplest example of which is just a "step", *i.e.*, one or several layers of HOPG break off and the layers below appear on the surface. The greater the height of such a step, the stronger the contrast change in the image. It can be expected that, in the vicinity of such topographic features at the edges of graphite layers in HOPG, the concentration of functional groups, primarily carbonyl and carboxyl, will be relatively high. On the other hand, the regions of the substrate between the inhomogeneities are atomically smooth graphite, the surface of which is highly inert, similar to that of carbon nanotubes and graphene. One can see from Fig. 2a that the precursor thin film uniformly covers both topographic defects *and* the atomically smooth inert part of the substrate. Images **b** and **c** present the patterns of the Pt nanoparticles obtained on the surface after thermal decomposition of the precursor (image **b**) and subsequent treatment in a hydrogen flow (image **c**). One can see that the uniformity of the precursor distribution directly leads to the uniform distribution of Pt nanoparticles. Despite a certain tendency of the nanoparticles to decorate the graphite "steps", the atomically smooth parts of the substrate are modified quite uniformly. Further, the nanoparticles after hydrogen treatment demonstrate somewhat "sharper", more defined edges. This is due to the more complete conversion achieved under this set of conditions, which was also confirmed in the work by means of X-ray photoelectron spectroscopy.

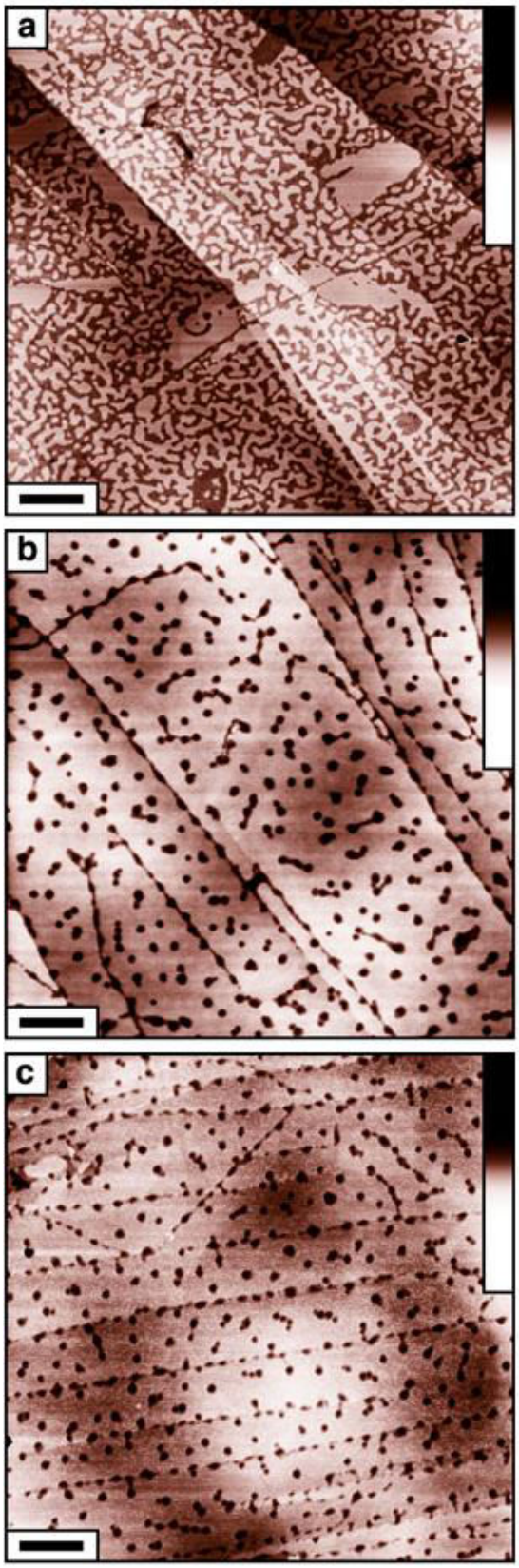


**Figure 2**. Typical AFM images of the structures on the HOPG surface. Image **a** refers to the precursor film after deposition; image **b** is the Pt nanoparticles formed after thermal destruction of the film; image **c** is the Pt nanoparticles formed after thermal destruction and subsequent post-processing in a hydrogen flow. The scale bar is 500 nm, the height scale is 30 nm. Reprinted with permission from Ref. [21].

Our further work [22] demonstrated that not only the model smooth inert surfaces but also dispersed ceramics, for example, titanium nitride, tin oxide, and silicon carbide can be decorated with Pt nanoparticles by means of SFDm. Such uniformity of deposition with respect to surfaces with very little or no "anchor" functional groups is achievable, arguably, precisely because of the absence of capillary forces and related effects at the stage of solvent removal. Indeed, it is known that in standard solvothermal approaches to the synthesis of Pt nanoparticles on the surface of carbon nanotubes or ceramics, the procedure of functionalization of these surfaces is routinely used. The problem here lays not so much in the difficulties with carrying out the functionalization process itself but in some ideological inconsistency that arises when functionalizing the surface of a material, one of the unique features of which is the high inertness of its surface.

As a final remark to the section, a possible approach to creating patterned metal nanoparticles by means of SFDm is considered. It is known that if the distance between the nanoparticles of an electrocatalytic material can be controlled, it should slow the degradation of the material *via* the particle coalescence scenario [23]. And yet, the use of SFDm alone does not provide an opportunity for regular organization of nanoparticles on the surface, only for their uniform deposition. However, we have demonstrated [24] that, if an organometallic precursor is dissolved in hydrogen-enriched $CO_2$ along with an amphiphilic copolymer forming micelles in sc $CO_2$, the patterned metal nanoparticles are organized on the surface of a substrate after autoclave decompression. Apparently, while a precursor is being chemically transformed, it loses its solubility in sc $CO_2$. The metal nanoparticles being formed in the process are still surrounded by some hydrocarbon ligand and, thus, have an affinity towards a hydrocarbon "core" of the micelle. As a result, the clusters of metal nanoparticles are encapsulated in the micelles and, after deposition on the surface, the minimal distance between the nanoparticle clusters is set. Any traces of the micelles can be removed through annealing that leaves a substrate with only patterning metal nanoparticles on its surface (see Fig. 3.).

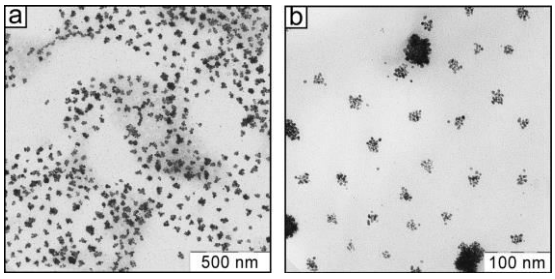


**Figure 3**. TEM images of the Pt nanoparticles with the controlled spacing between clusters deposited onto the model smooth surface using sc $CO_2$. Reprinted with permission from Ref. [24].

## Metal oxide nanoparticles and aerogels

Finely dispersed porous transition metal oxides are of great interest as materials for use in catalysis, sorption processes, and electrochemistry [25, 26]. The "classical" SFDm approach can be applied for transition metal organometallic composites as precursors with an annealing procedure in the presence of oxygen that yields the corresponding oxides. Yang and colleagues demonstrated [27–29] that the method can be implemented to decorate vertically aligned carbon nanotubes (VACNT) with cobalt, iron and nickel oxides. The proposed application for the resulting materials is the electrodes of supercapacitors since the materials feature high specific capacitance values ranging from 248 F $g^{-1}$ to 1088 F $g^{-1}$. From the standpoint of this review, it is worth mentioning that the uniform deposition of metal oxide nanoparticles on VACNT seems to be a perfect example of the benefits to be gained from using a supercritical fluid. Indeed, the VACNT morphology can be described as a carbon nanotube "forest" with nanometer-sized cylindrical pores stretching throughout the substrate. Thus, the use of a liquid rather than a supercritical medium should cause particular difficulties with both wetting the surface at the deposition stage and the residual solvent present in the pores after the solvent removal stage.

The modified SFDm method for supported metal oxides synthesis with both precursor and oxidant being dissolved in sc $CO_2$ can also be applied [30, 31]. Gougousi *et al*. [30] reported the formation of manganese, aluminum, zinc, ruthenium, hafnium and yttrium oxides using, among others, acetonitrile-, fluorinated acetylacetonate- and cyclopentadienyl-based precursors. Hydrogen peroxide in water or a solution of *tert*-butyl peroxyacetate in alcohol was used as an oxidant. The work presents an interesting example of SFDm implementation for the formation of thin films rather than nanoparticles, which can be beneficial if a "delicate" substrate (that can be easily damaged by conventional methods of surface modification by chemical vapor deposition or etching) is used. Crowley *et al.* [31] explored the same benefits of sc $CO_2$ in order to grow arrays of cobalt, copper and iron oxide nanowires and nanotubes inside mesoporous silica. This work presents an important example of organometallic precursors being decomposed to form metal oxide aerogels directly in sc $CO_2$ without any additional oxidant in an autoclave.

Our group demonstrated that, apart from using an additional annealing step or adding an oxidant that is liquid under normal conditions, the thermal decomposition of organometallic compounds in oxygen-enriched $CO_2$ can be used to obtain finely dispersed metal oxide nanoparticles [32]. The SEM images of manganese oxide nanoparticles produced in the described process using manganese cyclopentadienyl tricarbonyl as a precursor are presented in Fig. 4. Apparently, a rather narrow size distribution can be achieved due to the stabilization of the growing nanoparticles with a hydrocarbon shell derived from the cyclopentadienyl ligand. The electron conductivity of the nanoparticles was rather low as expected; therefore, for the electrocatalytic measurements, the synthesized material was mixed with carbon black. The cyclic voltammograms obtained for the materials revealed relatively high electrocatalytic efficiency for the oxygen reduction reaction in an alkaline medium comparable to that of Pt-based materials.

This work was followed by the study of the thermal decomposition of manganese carbonyl in oxygen-enriched sc $CO_2$ [33]. In this case, a somewhat unexpected result was obtained: the process of thermal decomposition of the carbonyl leads to the formation of monolithic aerogel-like structures rather than dispersed nanoparticles in an autoclave (see Fig. 5).

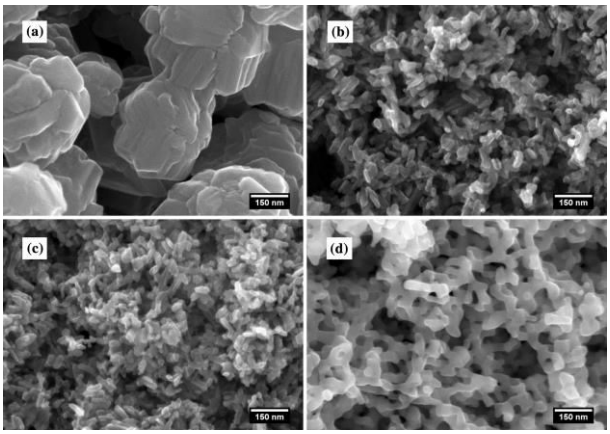


**Figure 4.** SEM images of the manganese oxide nanoparticles produced *via* thermal decomposition of cyclopentadienylmanganese tricarbonyl: in pure oxygen (**a**), in oxygen-enriched $CO_2$ (**b**, **c**), in oxygen-enriched $CO_2$ with subsequent annealing (**d**). Reprinted with permission from Ref. [32].

The X-ray diffraction (XRD) patterns indicated that the formed nanoparticles are amorphous. With the introduction of an additional annealing step, the nanoparticle sizes increase, while their specific surface area decreases from ≈170 $m^2$ $g^{-1}$ to ≈70 $m^2$ $g^{-1}$. The XRD spectra suggest that an orthorhombic $Mn_2O_3$ phase is formed after the annealing. Both a decrease in the specific surface area and an increase in the particle sizes indicate that the initial morphology of the manganese oxide nanoparticles formed in the described process is similar to that of the "classical" silica aerogels with nanometer-scale grains interconnecting to form larger particles.

Aerogels of various chemical nature are of great interest as the materials for electrochemical applications. The recent review by Alwin and Sahaya Shajan provides an extensive analysis of the literature on aerogels as materials for energy storage and conversion [34]: silica-, metal oxide-, metal- and bimetal-, organic- and carbon aerogels are considered. The most common general approach to aerogels synthesis consists of two main steps: the formation of a gel *via* a sol-gel procedure and removing liquid solvent from the gel without damaging the resulting 3D-structure. In particular, for the synthesis of metal oxide aerogels, including manganese oxide aerogels, the epoxy-initiated gelation developed by Gash *et al*. is usually implemented at the first step [35–37]. The technique uses metal salts rather than alkoxides as precursors and epoxides as proton scavengers. It was a breakthrough in the synthesis of metal oxide aerogels that allowed the formation of robust, mechanically stable materials with fine-tuned structures. However, this method involves a multicomponent process that requires a substantial amount of time: from several days up to several weeks. Therefore, a one-step process of metal oxide formation presented in Ref. [33] seems to be of certain importance. The process does not require any additives that are liquid under ambient conditions and takes only several hours. The preliminary experimental study performed by the group of Gallyamov *et al*. suggests that the tendency to form branched 3D-agglomerates during thermal decomposition in oxygen-enriched $CO_2$ is a common feature for many transition metal carbonyls. However, further research is required to gain insight into this field.

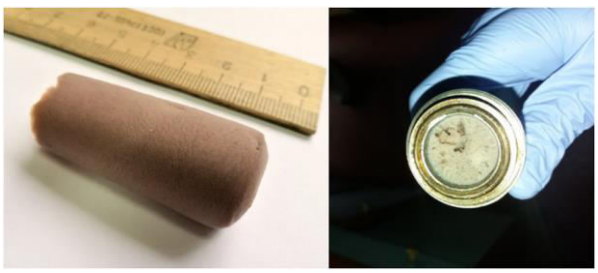

**Figure 5.** Photographs of the manganese oxide aerogel formed in an autoclave during thermal decomposition of manganese carbonyl in oxygen-enriched sc $CO_2$. Left image presents the aerogel after it was removed from the autoclave, right image demonstrates the aerogel in the autoclave. Reprinted with permission from Ref. [33].

## Modification of membranes

Ion-conducting polymer membrane (ICPM) is an integral part of most of electrochemical energy conversion devices, such as some of the fuel cell types, vanadium redox flow batteries, and lithium-based batteries. Selective ion conductivity, thermal, mechanical, and chemical stability should be combined for an optimal ICPM. Sc $CO_2$ can be used in both membrane preparation (usually as an anti-solvent [38]) and modification [39]. Our recent work [39] reviews the membrane modifications using sc $CO_2$ specifically for electrochemical applications. The present review is focused on the preparation of composite ICPM that contain inorganic nanoparticles and include recent works that were not analyzed in Ref. [39].

There are two main motifs for the development of composite ICPM that contain inorganic nanoparticles. The first one is the implementation of the self-humidifying polymer electrolyte membrane concept proposed by Watanabe *et al.* [40]. Briefly, if catalytic metal nanoparticles, such as Pt or Pd, are added to a membrane based on fluorinated polymeric sulfuric acid, such as Nafion, gas crossover through the membrane in a hydrogen/oxygen fuel cell will lead to the formation of water molecules in the membrane bulk. Since the presence of water is essential for ion conductivity of Nafion, the use of the self-humidifying composite membrane will allow such a fuel cell to operate without an external humidifying system. Further, for the direct methanol fuel cells, the addition of Pd particles suppresses methanol crossover as well. Erkey *et al.* suggested the SFDm approach for the modification of the Nafion membrane as an alternative to conventional chemical deposition methods [41]. Kim *et al.* suggested the use of Pd(II) acetylacetonate instead of Pd(II) hexafluoroacetylacetonate with a different reduction route [42]. Iwai *et al.* followed up with a thorough study on the effect of the precursor type and concentration in an autoclave [43] on the properties of the resulting Pd/Nafion composite membranes.

The second approach is associated with incorporation of inorganic nanoparticles into a polymer membrane in order to increase its selectivity, electrolyte uptake, and mechanical properties. Here, the nanoparticles, such as silica, metal oxides or zeolites, act as a steric barrier for the undesired reactant crossover through membrane, while their hygroscopic properties allow for an increase in the electrolyte or water uptake. Conventionally, to prepare such a composite, the Nafion membrane is immersed in the water/alcohol solution of an organic $SiO_2$ precursor and, then, the hydrolysis and condensation of the precursor inside the membrane is catalyzed

by $SO_3H$ groups of Nafion [44]. Su and colleagues suggested using sc $CO_2$ as a medium that both swells the Nafion membrane and dissolves the $SiO_2$ precursor [45, 46]. Su *et al.* demonstrated that the resulting composite membrane has the suppressed methanol crossover and higher selectivity for use in direct methanol fuel cells. Simonov *et al.* confirmed that the modification leads to an increase in the water uptake and tested the composite membranes as separators for vanadium redox flow batteries (VRFB) [47]. Sizov *et al.* suggested somewhat different modification with tungsten oxide nanoparticles formed inside the Nafion membrane *via* thermal decomposition of tungsten carbonyl [48]. The incorporation of $WO_X$ nanoparticles decreased the vanadyl ion crossover through the membrane with little effect on the proton conductivity.

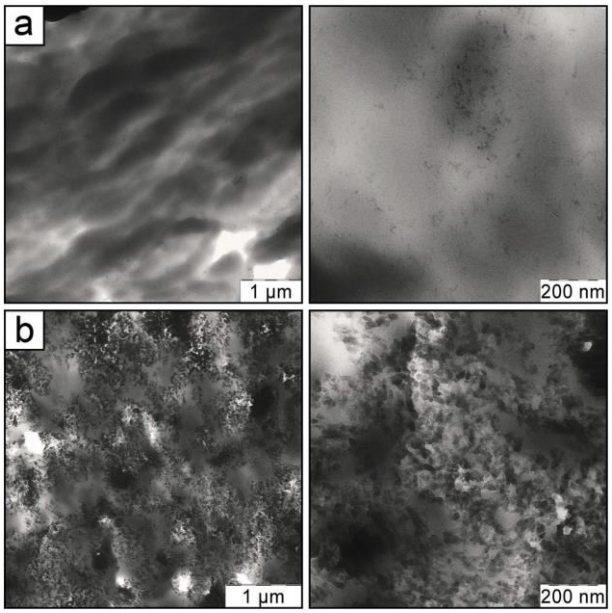


**Figure 6.** TEM images of the polyolefin–silica composite membranes prepared using sc $CO_2$ as a medium. Row **a**: lower precursor concentration; row **b**: higher precursor concentration. Reprinted with permission from Ref. [49].

The described modifications of the Nafion membrane are aimed at tailoring its properties for the desired electrochemical application. However, a major problem of the high cost of perfluorinated polysulfonic acid membranes should also be addressed. Sizov *et al.* [49] proposed a novel polyolefin–silica composite membrane for use in VRFB. Here, the organic silica precursor is delivered inside the pores of the polyolefin membranes using sc $CO_2$ as a solvent. The pores are pre-wetted with water, and the hydrolysis and condensation of the precursor are catalyzed by carbonic acid that results from the interaction of water with carbon dioxide under pressure. Alkoxysilanes were used as precursors, and, in that sense, the mentioned work [49] follows the methodology of alkoxysilane chemistry in biphase $H_2O/CO_2$ media developed by Kalinina *et al.* [50, 51]. Sizov *et al.* demonstrated that the sizes of silica particles can be controlled by the amount of an alkoxysilane precursor added to the autoclave (see Fig. 6). Although the proton conductivity of the modified membrane is significantly lower than that of Nafion, the selectivity is comparable. Considering the fact that the polyolefin membrane is several orders of magnitude cheaper than Nafion, the results obtained seem to be promising and this approach has much room for further development.

## Conclusions

The synthesis and modification of functional materials for electrochemical applications is an important niche for use of sc $CO_2$ as a medium. The absence of capillary effects, characteristic of a supercritical fluid, enables efficient modification of porous media of various chemical nature: from electron-conducting carbon-based substrates to polymer ion-conducting membranes. More specifically, for the preparation of supported noble metal electrocatalytic nanoparticles, a thin film of an organometallic precursor can be uniformly deposited from solutions in sc $CO_2$ onto dispersed supports, including those with highly inert surfaces, such as carbon nanotubes or ceramics. The subsequent conversion of the precursor leads to the uniform distribution of metal nanoparticles on the surface. This uniformity can decrease the degradation rate due to the suppressed coalescence mechanism. For the synthesis of metal oxide nanoparticles, the thermal decomposition of organometallic precursors can be performed directly in oxygen-enriched sc $CO_2$, yielding a rather monodisperse electrocatalyst for the oxygen reduction in an alkaline media. When manganese carbonyl is used as a precursor, a monolithic aerogel-like material is formed. Potentially, this can expand the use of sc $CO_2$ for the preparation of metal oxide aerogels beyond a mere supercritical drying tool. Both perfluorinated polysulfonic acid and inert polyolefin membranes can be modified with metal, metal oxide and silica inorganic nanoparticles using sc $CO_2$ as a solvent for the corresponding precursors. The high permeability of sc $CO_2$ as well as its ability to swell certain polymers lead to a uniform distribution of inorganic nanoparticles throughout the membrane bulk.

## Acknowledgements

The reported study was funded by the Russian Foundation for Basic Research, project nos. 18-29-06036_mk and 20-33-70220. This work was supported by the Ministry of Science and Higher Education of the Russian Federation.

## Corresponding author

* E-mail: elmanovich@polly.phys.msu.ru (I. V. Elmanovich)

## References

1. J. J. Watkins, T. J. McCarthy, *Chem. Mater.*, **1995**, *7*, 1991–1994. DOI: 10.1021/cm00059a001
2. K. S. Morley, P. C. Marr, P. B. Webb, A. R. Berry, F. J. Allison, G. Moldovan, P. D. Brown, S. M. Howdle, *J. Mater. Chem.*, **2002**, *12*, 1898–1905. DOI: 10.1039/b111111f
3. T. E. Grigor'ev, E. E. Said-Galiev, A. Yu. Nikolaev, M. S. Kondratenko, I. V. Elmanovich, M. O. Gallyamov, A. R. Khokhlov, *Nanotechnol. Russ.*, **2011**, *6*, 311–322. DOI: 10.1134/S1995078011030062
4. S. E. Bozbag, N. S. Yasar, L. C. Zhang, M. Aindow, C. Erkey, *J. Supercrit. Fluids*, **2011**, *56*, 105–113. DOI:

10.1016/j.supflu.2010.10.045

5. X. R. Ye, Y. Lin, C. M. Wai, *Chem. Commun.*, **2003**, 642–643. DOI: 10.1039/b211350c
6. X.-R. Ye, Y. Lin, C. Wang, M. H. Engelhard, Y. Wang, C. M. Wai, *J. Mater. Chem.*, **2004**, *14*, 908–913. DOI: 10.1039/b308124a
7. R. K. Boggess, L. T. Taylor, D. M. Stoakley, A. K. St. Clair, *J. Appl. Polym. Sci.*, **1997**, *64*, 1309–1317. DOI: 10.1002/(sici)1097-4628(19970516)64:7<1309::aid-app10>3.3.co;2-7
8. Q. Peng, J. C. Spagnola, G. N. Parsons, *J. Electrochem. Soc.*, **2008**, *155*, D580–D582. DOI: 10.1149/1.2946723
9. A. Bayrakçeken, B. Cangül, L. C. Zhang, M. Aindow, C. Erkey, *Int. J. Hydrogen Energy*, **2010**, *35*, 11669–11680. DOI: 10.1016/j.ijhydene.2010.08.059
10. Y. Zhang, C. Erkey, *J. Supercrit. Fluids*, **2006**, *38*, 252–267. DOI: 10.1016/j.supflu.2006.03.021
11. M. Türk, C. Erkey, *J. Supercrit. Fluids*, **2018**, *134*, 176–183. DOI: 10.1016/j.supflu.2017.12.010
12. S. B. Barim, E. Uzunlar, S. E. Bozbag, C. Erkey, *J. Electrochem. Soc.*, **2020**, *167*, 054510. DOI: 10.1149/1945-7111/ab68d1
13. H. A. Gasteiger, S. S. Kocha, B. Sompalli, F. T. Wagner, *Appl. Catal.*, *B*, **2005**, *56*, 9–35. DOI: 10.1016/j.apcatb.2004.06.021
14. C. D. Saquing, T.-T. Cheng, M. Aindow, C. Erkey, *J. Phys. Chem. B.*, **2004**, *108*, 7716–7722. DOI: 10.1021/jp049535v
15. Y. Lin, X. Cui, X. Ye, *Electrochem. Commun*., **2005**, *7*, 267–274. DOI: 10.1016/j.elecom.2005.01.007
16. A. Smirnova, X. Dong, H. Hara, A. Vasiliev, N. Sammes, *Int. J. Hydrogen Energy*, **2005**, *30*, 149–158. DOI: 10.1016/j.ijhydene.2004.04.014
17. A. Bayrakçeken, A. Smirnova, U. Kitkamthorn, M. Aindow, L. Türker, İ. Eroğlu, C. Erkey, *J. Power Sources*, **2008**, *179*, 532–540. DOI: 10.1016/j.jpowsour.2007.12.086
18. S. E. Bozbag, T. Gümüşoglu, S. Yilmaztürk, C. J. Ayala, M. Aindow, H. Deligöz, C. Erkey, *J. Supercrit. Fluids*, **2015**, *97*, 154–164. DOI: 10.1016/j.supflu.2014.08.014
19. E. E. Said-Galiyev, A. Yu. Nikolaev, E. E. Levin, E. K. Lavrentyeva, M. O. Gallyamov, S. N. Polyakov, G. A. Tsirlina, O. A. Petrii, A. R. Khokhlov, *J. Solid State Electrochem.*, **2011**, *15*, 623–633. DOI: 10.1007/s10008-010-1169-7
20. J. D. Wnuk, J. M. Gorham, S. G. Rosenberg, W. F. van Dorp, T. E. Madey, C. W. Hagen, D. H. Fairbrother, *J. Appl. Phys.*, **2010**, *107*, 054301. DOI: 10.1063/1.3295918
21. I. V. Elmanovich, A. V. Naumkin, M. O. Gallyamov, A. R. Khokhlov, *J. Nanopart. Res.*, **2012**, *14*, 733. DOI: 10.1007/s11051-012-0733-8
22. I. V. Elmanovich, V. V. Zefirov, M. O. Gallyamov, A. R. Khokhlov, *Dokl. Phys. Chem.*, **2017**, *473*, 41–44. DOI: 10.1134/S0012501617030010
23. J. C. Meier, C. Galeano, I. Katsounaros, J. Witte, H. J. Bongard, A. A. Topalov, C. Baldizzone, S. Mezzavilla, F. Schüth, K. J. J. Mayrhofer, *Beilstein J. Nanotechnol.*, **2014**, *5*, 44–67. DOI: 10.3762/bjnano.5.5
24. D. O. Kolomytkin, I. V. Elmanovich, S. S. Abramchuk, L. A. Tsarkova, D. Pospiech, M. Möller, M. O. Gallyamov, A. R. Khokhlov, *Eur. Polym. J.*, **2015**, *71*, 73–84. DOI: 10.1016/j.eurpolymj.2015.07.048
25. Y. Wang, J. Li, Z. Wei, *J. Mater. Chem. A*, **2018**, *6*, 8194–8209. DOI: 10.1039/C8TA01321G
26. A. Akbari, M. Amini, A. Tarassoli, B. Eftekhari-Sis, N. Ghasemian, E. Jabbari, *Nano-Struct. Nano-Objects*, **2018**, *14*, 19–48. DOI: 10.1016/j.nanoso.2018.01.006
27. J. Cheng, B. Zhao, W. Zhang, F. Shi, G. Zheng, D. Zhang, J. Yang, *Adv. Funct. Mater.*, **2015**, *25,* 7381–7391. DOI: 10.1002/adfm.201502711
28. W. Zhang, B. Zhao, Y. Yin, T. Yin, J. Cheng, K. Zhan, Y. Yan, J. Yang, J. Li, *J. Mater. Chem. A*, **2016**, *4*, 19026–19036. DOI: 10.1039/c6ta07720j
29. Y. Yin, Y. Xu, Y. Zhou, Y. Yan, K. Zhan, J. Yang, J. Li, B. Zhao, *ChemElectroChem*, **2018**, *5*, 1394–1400. DOI: 10.1002/celc.201800138
30. T. Gougousi, D. Barua, E. D. Young, G. N. Parsons, *Chem. Mater.*, **2005**, *17*, 5093–5100. DOI: 10.1021/cm0510965
31. T. A. Crowley, K. J. Ziegler, D. M. Lyons, D. Erts, H. Olin, M. A. Morris, J. D. Holmes, *Chem. Mater*., **2003**, *15*, 3518–3522. DOI: 10.1021/cm034139v
32. V. V. Zefirov, I. V. Elmanovich, E. E. Levin, S. S. Abramchuk, *J. Mater. Sci.*, **2018**, *53*, 9449–9462. DOI: 10.1007/s10853-018-2242-3
33. V. V. Zefirov, I. V. Elmanovich, A. V. Pastukhov, E. P. Kharitonova, A. A. Korlyukov, M. O. Gallyamov, *J. Sol-Gel Sci. Technol*., **2019**, *92*, 116–123. DOI: 10.1007/s10971-019-05092-2
34. S. Alwin, X. Sahaya Shajan, *Mater. Renewable Sustainable Energy*, **2020**, *9*, 7. DOI: 10.1007/s40243-020-00168-4
35. A. E. Gash, T. M. Tillotson, J. H. Satcher, J. F. Poco, L. W. Hrubesh, R. L. Simpson, *Chem. Mater.*, **2001**, *13*, 999–1007. DOI: 10.1021/cm0007611
36. T. F. Baumann, A. E. Gash, S. C. Chinn, A. M. Sawvel, R. S. Maxwell, J. H. Satcher, *Chem. Mater.*, **2005**, *17*, 395–401. DOI: 10.1021/cm048800m
37. M. Davis, C. Gümeci, C. Kiel, L. J. Hope-Weeks, *J. Sol-Gel Sci. Technol.*, **2011**, *58*, 535–538. DOI: 10.1007/s10971-011-2424-9
38. A. Figoli, T. Marino, S. Simone, E. Di Nicolò, X.-M. Li, T. He, S. Tornaghi, E. Drioli, *Green Chem.*, **2014**, *16*, 4034–4059. DOI: 10.1039/c4gc00613e
39. M. S. Kondratenko, I. V. Elmanovich, M. O. Gallyamov, *J. Supercrit. Fluids*, **2017**, *127*, 229–246. DOI: 10.1016/j.supflu.2017.03.011
40. M. Watanabe, H. Uchida, Y. Seki, M. Emori, P. Stonehart, *J. Electrochem. Soc.*, **1996**, *143*, 3847–3852. DOI: 10.1149/1.1837307
41. R. Jiang, Y. Zhang, S. Swier, X. Wei, C. Erkey, H. R. Kunz, J. M. Fenton, *Electrochem. Solid-State Lett.*, **2005**, *8*, A611. DOI: 10.1149/1.2050527
42. D. Kim, J. Sauk, J. Byun, K. S. Lee, H. Kim, *Solid State Ionics*, **2007**, *178*, 865–870. DOI: 10.1016/j.ssi.2007.02.034
43. Y. Iwai, S. Ikemoto, K. Haramaki, R. Hattori, S. Yonezawa, *J. Supercrit. Fluids*, **2014**, *94*, 48–58. DOI: 10.1016/j.supflu.2014.06.015
44. R. Jiang, H. R. Kunz, J. M. Fenton, *J. Membr. Sci.*, **2006**, *272*, 116–124. DOI: 10.1016/j.memsci.2005.07.026
45. L. Su, L. Li, H. Li, J. Tang, Y. Zhang, W. Yu, C. Zhou, *J. Power Sources*, **2009**, *194*, 220–225. DOI: 10.1016/j.jpowsour.2009.04.070
46. L. Su, S. Pei, L. Li, H. Li, Y. Zhang, W. Yu, C. Zhou, *Int. J. Hydrogen Energy*, **2009**, *34*, 6892–6901. DOI: 10.1016/j.ijhydene.2009.05.145
47. A. S. Simonov, M. S. Kondratenko, I. V. Elmanovich, V. E. Sizov, E. P. Kharitonova, S. S. Abramchuk, A. Yu. Nikolaev, D. A. Fedosov, M. O. Gallyamov, A. R. Khokhlov, *J. Membr. Sci.*, **2018**, *564*, 106–114. DOI: 10.1016/j.memsci.2018.06.042
48. V. E. Sizov, V. V. Zefirov, S. S. Abramchuk, A. A. Korlyukov, M. S. Kondratenko, V. G. Vasil'ev, M. O. Gallyamov, *J. Membr. Sci*., **2020**, *609*, 118244. DOI: 10.1016/j.memsci.2020.118244
49. V. V. Zefirov, V. E. Sizov, M. S. Kondratenko, I. V. Elmanovich, S. S. Abramchuk, V. G. Sergeyev, M. O. Gallyamov, *J. Supercrit. Fluids*, **2019**, *150*, 56–64. DOI: 10.1016/j.supflu.2019.04.015
50. A. A. Kalinina, I. V. Elmanovich, M. N. Temnikov, M. A. Pigaleva, A. S. Zhiltsov, M. O. Gallyamov, A. M. Muzafarov, *RSC Adv.*, **2015**, *5*, 5664–5666. DOI: 10.1039/C4RA13619E
51. A. A. Kalinina, D. N. Kholodkov, I. B. Meshkov, M. A. Pigaleva, I. V. Elmanovich, Y. A. Molodtsova, M. O. Gallyamov, A. M. Muzafarov, *Russ. Chem. Bull.*, **2016**, *65*, 1104–1109. DOI: 10.1007/s11172-016-1419-7